



## WEDNESDAY SLIDE CONFERENCE 2012-2013

# Conference 6

17 October 2012

---

**CASE I:** Stanford 1 (JPC 4019361).

**Signalment:** 4-month-old, female, C57BL/6 mouse (*Mus musculus*).

**History:** This mouse received a single 400 mg/kg dose of acetaminophen (suspension in PBS) by oral gavage. The mouse was sacrificed 24 hours after.

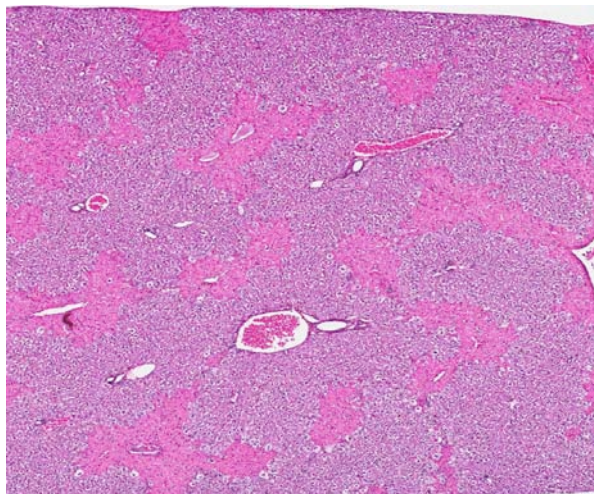
**Gross Pathology:** This mouse is presented alive in good body condition. There is mild, diffuse, red and

tan mottling of the liver. All other organs and tissues are within normal gross limits.

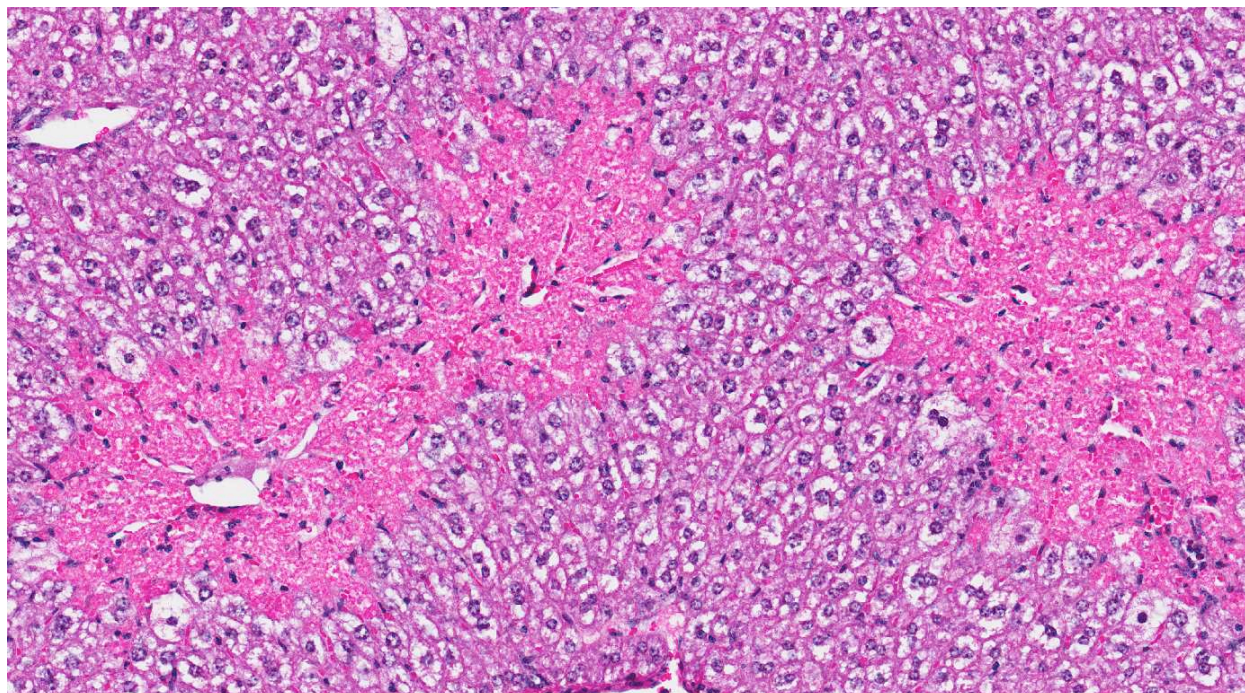
**Histopathologic Description:** Multiple sections of liver are examined, revealing moderate acute hepatocellular necrosis of hepatocytes around central veins (centrilobular necrosis; zone III necrosis). The necrosis is coagulative in nature, characterized by hypereosinophilia and swelling of affected hepatocytes with karyolysis and rarely pyknosis and/or karyorrhexis. Rare scattered individual hepatocytes throughout the liver are condensed, hypereosinophilic, round with absent nuclei (interpreted as apoptosis; Councilman bodies). Diffusely, remaining hepatocytes in other areas/zones are mildly swollen due to intracellular accumulation of small to moderate amounts of small- to medium-sized, clear, round vacuoles (interpreted as microvesicular lipid droplets).

**Contributor's Morphologic Diagnosis:** 1. Liver, centrilobular necrosis, diffuse, moderate, acute.  
2. Liver, microvesicular hepatic lipidosis, diffuse, mild.

**Contributor's Comment:** Acetaminophen (APAP; paracetamol) is a nonprescription drug used in humans. APAP is an aniline analgesic, and at therapeutic doses (500-1000 mg per human tid/qid), it has similar analgesic and antipyretic effects as ibuprofen and aspirin.<sup>2,3</sup> However, it is not classified as a NSAID anti-inflammatory agent because it is a weak COX inhibitor.<sup>2,3</sup>



1-1. Liver, mouse: A reticular pattern of eosinophilic coagulative necrosis surrounds centrilobular veins diffusely throughout the section. (HE 33X)



1-2. Liver, mouse: Higher magnification of a focus of centrilobular necrosis characterized by maintenance of hepatic architecture granular eosinophilic cytoplasm, and hypertrophy of Kupffer and endothelial cell nuclei. (HE 164X)

In most mammalian species (including humans, mice and dogs), the biotransformation of APAP involves conjugation with glucuronic acid or sulfate in the liver, which are subsequently excreted by urinary system.<sup>1,2,3,4,7</sup> A small amount of APAP is metabolized by the P-450 (CYP) system to the reactive metabolite N-acetyl *p*-benzoquinone imine (NAPQI) in centrilobular zone hepatocytes, which is subsequently scavenged by glutathione.<sup>2,3,4,5,6</sup>

APAP toxicity manifests primarily as centrilobular hepatic necrosis that can lead to acute liver failure. In humans, a single or accumulative daily toxic dose is usually >15-25 g.<sup>2,3,4</sup> The mechanism of APAP hepatotoxicity is as follows:<sup>2,3,5,6</sup>

1. At toxic doses, increased metabolism of APAP by the P-450 (CYP) system leads to higher concentrations of NAPQI formation in centrilobular zone hepatocytes.
2. Higher concentrations of NAPQI deplete glutathione concentrations in centrilobular zone hepatocytes, leading to increased formation of reactive oxygen and nitrogen species.
3. Increased oxidative stress in centrilobular zone hepatocytes results in alterations in calcium homeostasis and initiation of mitochondrial permeability transition.
4. Loss of mitochondrial membrane potential in mitochondria of centrilobular zone

hepatocytes leads to loss of ATP synthesis subsequent necrosis.

Antidotes that can prevent or ameliorate APAP toxicity aim to prevent the loss/promote the synthesis of glutathione, such as with cysteine and methionine administration.<sup>2,3,4</sup>

Cats are more sensitive to APAP toxicity and have a different pattern of APAP toxicity due to a species deficiency in glucuronyl transferase, resulting in relatively higher conversion rates of APAP to the reactive NAPQI metabolite.<sup>1,7</sup> In addition to depleting glutathione in centrilobular hepatocytes, NAPQI can also deplete glutathione in erythrocytes, leading to methemoglobinemia, Heinz body hemolytic anemia, and methemoglobinuria.<sup>1,7</sup>

Currently, APAP toxicity is the leading cause of liver failure in humans in the US and UK. Since APAP biotransformation and toxicity is similar between humans and mice, this makes mice an attractive and clinically relevant animal model for research into acetaminophen hepatotoxicity and other toxicities leading to centrilobular necrosis of the liver via the P-450 (CYP) system.<sup>2,4</sup>

**JPC Diagnosis:** Liver, centrilobular hepatocytes: Necrosis, coagulative, diffuse.

**Conference Comment:** The contributor provided a very good summary of acetaminophen (APAP; paracetamol) toxicity. During the discussion of this

case, the moderator stressed the importance of phase 1 and phase 2 drug metabolism. Xenobiotics (chemicals not normally found or expected to be in the body) can undergo metabolism via various pathways, with the ultimate endpoint being excretion of water soluble metabolites through urine or bile. Many xenobiotic drugs are lipid-soluble and therefore pose a challenge to such excretion. Thus, a critical step in xenobiotic metabolism is the formation of water-soluble metabolites. Phase 1 drug metabolism includes oxidation, reduction and hydrolysis by various enzyme systems. If the resulting compound is sufficiently water soluble, then it is excreted via the kidneys or bile; however, if phase 1 does not render the drug excretable, it undergoes phase 2 metabolism. Phase 2 metabolism involves conjugation with ionized groups to significantly increase its water solubility and thus further enhance its excretion. Examples of phase 2 conjugation reactions include glucuronidation, sulphation, acetylation and methylation.<sup>8</sup>

Drug metabolism occurs at several sites, including liver, intestines, lung, kidney, and plasma with the liver being the primary site. The liver contains a relatively large percentage of the body's metabolizing enzymes, most importantly a group of proteins known as cytochrome P450 mixed function oxidases. These enzymes are found within microsomes in the smooth endoplasmic reticulum of centrilobular hepatocytes. The most common reaction catalyzed by the cytochrome P450 enzymes is a mono-oxygenase reaction in which a molecule of oxygen (O<sub>2</sub>) is split, with one oxygen atom oxidizing the xenobiotic and reduction of the other oxygen atom to produce a molecule of water. This oxidation-reduction reaction is responsible for the metabolism of a variety of drugs, to include paracetamol. Cytochrome P450 enzymes also catalyze reduction reactions to metabolize drugs such as prednisone, warfarin, and halothane. The third type of phase 1 metabolism reaction is hydrolysis, which is catalyzed by esterases and amidases (which also occur in hepatocytes and other extrahepatic sites, including plasma).<sup>8</sup>

Of the phase 2 reactions, glucuronidation and sulphation play a major role in the metabolism of paracetamol, with approximately 40% of the drug undergoing each reaction. As the contributor states, a small amount of paracetamol undergoes phase 1 N-hydroxylation which results in the toxic product N-acetyl-p-amino-benzoquinoneimine which is normally further metabolized (conjugated) by glutathione.<sup>8</sup>

Further discussion on this case centered on the use of severity modifiers ("mild," "moderate," "severe") to quantify the extent of necrosis, which can be important in a case such as this in which there is a dose-dependent response. Toxicologic pathologists often

use such modifiers for quantification; however, this terminology is not traditionally used in diagnostic pathology at the AFIP/JPC, with the reasoning that necrosis in itself cannot be "mild" nor "severe".

**Contributing Institution:** Veterinary Services Center, Department of Comparative Medicine, Stanford School of Medicine (<http://med.stanford.edu/compmed/>)

#### References:

1. Court MH, Greenblatt DJ. Molecular basis for deficient acetaminophen glucuronidation in cats. *Biochem Pharmacol.* 1997;53:1041-1047.
2. Hinson JA, Roberts DW, James LP. Mechanisms of acetaminophen-induced liver necrosis. *Handb Exp Pharmacol.* 2010;196:369-405.
3. James LP, Mayeux PR, Hinson JA. Acetaminophen hepatotoxicity. *Drug Metab Disposition.* 2003;31:1499-1506.
4. Jaschke H, McGill MR, Williams CD, et al. Current issues with acetaminophen hepatotoxicity – a clinically relevant model to test the efficacy of natural products. *Life Sciences.* 2011;88:737-745.
5. Kumar V, Abbas AK, Fausto N. Cellular adaptation, cell injury, and cell death. In: Kumar V, Abbas AK, Fausto N, eds. *Robbins and Coltran Pathologic Basis of Disease.* 7<sup>th</sup> ed. Philadelphia, PA: Elsevier Saunders; 2005:25-26.
6. Maitra A, Kumar V. Environmental and nutritional pathology. In: Kumar V, Abbas AK, Fausto N, eds. *Robbins and Coltran Pathologic Basis of Disease.* 7<sup>th</sup> ed. Philadelphia, PA: Elsevier Saunders; 2005:424.
7. Savides MC, Oehme FW, Nash SL, et al. The toxicity and biotransformation of single doses of acetaminophen in dogs and cats. *Toxicol Appl Pharmacol.* 1984;74:26-34.
8. Schonborn JL, Gwinnett C. The role of the liver in drug metabolism. Anesthesia tutorial of the week 179. *ATOTW.* 2010(179):1-6. <http://www.aagbi.org/sites/default/files/179-The-role-of-the-liver-in-drug-metabolism.pdf>. Accessed 18 October 2012.

**CASE II:** 12-661 3 9 (JPC 4019358).

**Signalment:** 8-month-old, intact female, mouse, *Mus musculus*, B6.Cg-Tg(APP<sup>S</sup>wF1<sub>Lon</sub>,PSEN1\*<sup>M146L</sup>\*<sup>L286V</sup>)6799Vas/Mmjax.

**History:** The goal of this experiment was to test the efficacy of a novel compound. This mouse was in the control group and was administered the vehicle without the compound by subcutaneous injection. Mice were sacrificed at the end of the study and tissues were collected to assess the effect of the compound by histopathology and other methods.

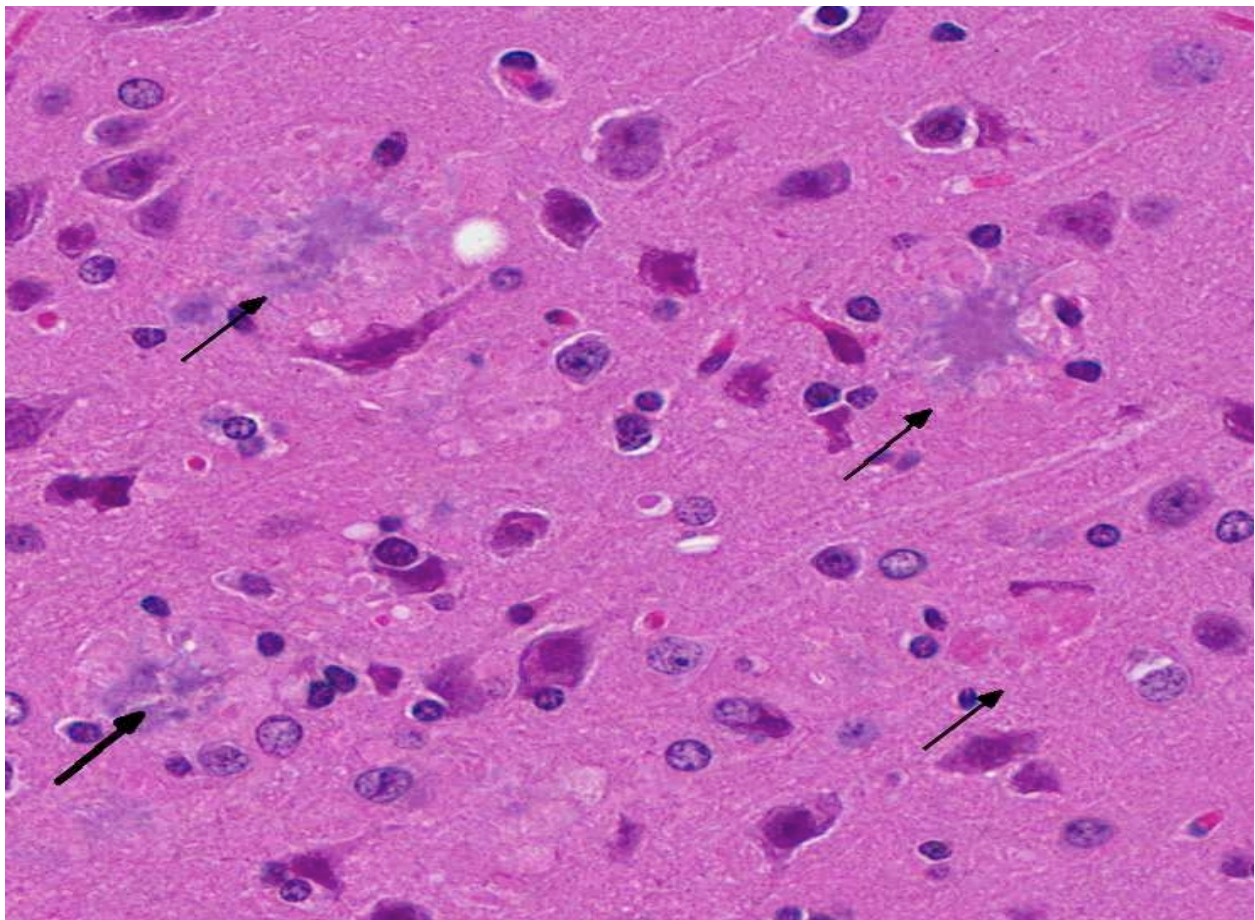
**Gross Pathology:** Complete necropsies were performed and no gross lesions were observed.

**Histopathologic Description:** Coronal sections of the head are provided, and include sections of the brain at the level of the cerebral cortex, hippocampus, thalamus, midbrain, and pituitary gland, and at the level of the cerebellum and brainstem. Multifocally in the neuropil of the cerebral cortex, hippocampus,

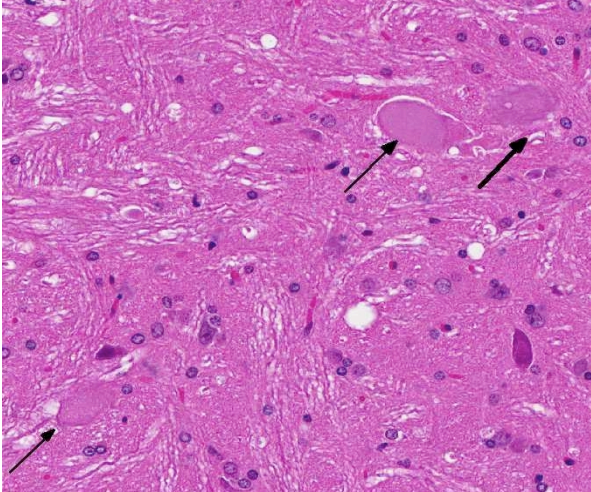
thalamus, and midbrain, there are numerous aggregates of a basophilic, amorphous to finely fibrillar material, which is often surrounded by a rim of decreased staining intensity of the neuropil. On Congo Red stain, this material is congophilic and shows green birefringence when observed with polarized light.

**Contributor's Morphologic Diagnosis:** Brain, cerebral cortex, hippocampus, thalamus, and midbrain: Abundant neuritic plaques with amyloid core, multifocal.

**Contributor's Comment:** The mouse strain B6.Cg-Tg(APP<sup>S</sup>wF1<sub>Lon</sub>,PSEN1\*<sup>M146L</sup>\*<sup>L286V</sup>)6799Vas/Mmjax is also known by the common names 5XFAD and Tg6799. This strain overexpresses two mutant human genes on a C57BL/6 and SJL background. The first gene, APP695, contains four mutations associated with familial Alzheimer's disease (FAD): the Swedish (K670N, M671L), Florida (I716V), and London (V717I) mutations. The second gene, PS1, contains two mutations also associated with FAD: M146L and L286V. Expression of both transgenes is regulated by neural-specific elements of the mouse Thy1 promoter



2-1. Brain, cerebrum, superficial cortex, B6.Cg-Tg(APP<sup>S</sup>wF1<sub>Lon</sub>,PSEN1\*<sup>M146L</sup>\*<sup>L286V</sup>)6799Vas/Mmjax mouse: There are numerous well-formed neuritic plaques (arrows) composed of beta-amyloid. (HE 230X)



2-2. Brain, cerebrum, superficial cortex, B6.Cg-Tg(APP<sup>SwFLon</sup>,PSEN1\*<sup>M146L</sup>\*<sup>L286V</sup>)6799Vas/Mmjax mouse: Multifocally, neurons within the brainstem nuclei exhibit central chromatolysis (arrows), neuronal cell body swelling, and axonal dilation (spheroid formation). (HE 320X)

to drive overexpression in the brain. This strain rapidly recapitulates the amyloid pathology of Alzheimer's disease (AD), beginning at 2 months of age and characterized by the formation of a heavy burden of neuritic plaques.<sup>1</sup> Neuritic plaques (also called senile plaques) are focal round collections of dilated and tortuous neurites that surround an amyloid core that can be stained with Congo Red.<sup>2</sup> Neuritic plaques are often surrounded by a clear halo and by reactive astrocytes and microglial cells. In humans, these plaques range in size from 20 to 200  $\mu\text{m}$  and are predominantly observed in the hippocampus, amygdala, and neocortex, with relative sparing of primary motor and sensitive cortices.

The main component of the amyloid core is A, a peptide derived from cleavage of the larger protein Amyloid Precursor Protein (APP), a cell surface protein that may function as a receptor.<sup>2</sup> The A peptides readily aggregate and can be directly neurotoxic and can result in synaptic dysfunction and an inflammatory response. Other proteins that present in plaques in smaller amounts include complement proteins, pro-inflammatory cytokines, 1-antichymotrypsin, and apolipoproteins. Findings in individuals affected by the familiar form of AD have supported the hypothesis that the generation of A is a critical step in the initiation of the disease. Some patients with familial AD have point mutations of the APP gene. Two other commonly affected loci are in the Presenilin 1 and 2 (PS1, PS2), which lead to a gain of function of the  $\gamma$ -secretase complex, which is involved in the cleavage of APP into A.

The other main morphologic change in AD is the formation of neurofibrillary tangles, which are composed of bundles of filaments in the cytoplasm of

neurons.<sup>2</sup> These are seen as basophilic structures by H&E staining, and can be demonstrated by silver stain methods such as Bielschowsky. A major component of these filaments is a hyperphosphorylated form of the protein tau. Tangles are not specific to AD, as they can be found in other diseases. There was no evidence of neurofibrillary tangles in the brain of these mice on H&E and Bielschowsky stains.

**JPC Diagnosis:** 1. Cerebrum, hippocampus, amygdaloid nucleus and brainstem: Neuritic plaques, numerous, diffuse, with gliosis and neuronal loss.

2. Brainstem nuclei and neurons: Chromatolysis, multifocal, marked, with spheroid formation.

**Conference Comment:** The contributor provided a thorough description of the components of the senile (neuritic) plaques and neurofibrillary tangles (NFT), the two microscopic hallmarks of Alzheimer's disease first described by Alois Alzheimer in 1906.<sup>3</sup> Senile plaques and NFTs represent two manifestations of abnormally folded A proteins.<sup>1</sup> Normally the body prevents such misfolded proteins from depositing in tissues and interfering with normal functions via several mechanisms collectively known as the "unfolded protein response" (UPR). The UPR activates signaling pathways that: 1) increase chaperone production in an attempt to repair, refold, and return proteins to normal; 2) slow protein translation; and 3) enhance the ubiquitination and proteasome pathway of misfolded proteins via the ubiquitin-proteasome pathway.<sup>1,4,5</sup> If the UPR is insufficient, abnormal proteins may be removed by autophagy, the major degradative pathway for intracellular components. Failure of autophagy has been implicated in the pathogenesis of several neurodegenerative diseases, including Alzheimer's disease.<sup>5</sup>

Three autophagic mechanisms are described in mammalian cells: chaperone-mediated autophagy, microautophagy, and macroautophagy, all which result in the lysosomal degradation of targeted cellular components. In chaperone-mediated autophagy, cytoplasmic proteins exposing a KFERQ-like motif are targeted directly to the lysosomes for degradation. Microautophagy involves the invagination of the lysosomal membrane to nonselectively engulf and degrade small portions of the cytoplasm. Macroautophagy is the best characterized mechanism of autophagy; thus, it is often referred to as simply "autophagy."

Unlike chaperone-mediated autophagy and microautophagy, macroautophagy relies on the *de novo* synthesis of double membrane-bound autophagosomes. The major upstream inhibitor of macroautophagy initiation is the mammalian target of rapamycin

complex 1 (mTORC1), which regulates several cellular processes, to include autophagy, cell growth and proliferation, and protein synthesis. Various cell signaling pathways converge upon mTORC1; for instance, in response to insulin and growth factors, the class I phosphatidylinositol-3-kinase (PI3K)/Akt signaling pathway activates mTORC1 and thus suppresses autophagy. Conversely, energy depletion signals through the liver kinase B1 (LKB1)/AMP-activated protein kinase (AMPK) pathway to inhibit mTORC1, and thereby activate autophagy.

When mTORC1 is inhibited, autophagy-related (Atg) proteins coordinate a series of events that results in the formation of an autophagosome (i.e., vesicle nucleation, vesicle elongation, docking and fusion, and vesicle maturation). This series begins with the formation of a phagophore (i.e., pre-autophagosomal structure) and progresses to the formation of a double membrane enclosed autophagosome, the outer membrane of which fuses with a lysosome or a late endosome to form an autolysosome or an amphisome, respectively. Acidic hydrolases digest material within the autolysosome or amphisome, after which the lysosome is restored.<sup>5</sup>

Current research strongly suggests the disruption of proteolysis within autolysosomes is the principle mechanism underlying autophagy failure in Alzheimer's disease. Various forms of autophagic vacuoles representing intermediate stages in autophagy (including autophagosomes, amphisomes, and autolysosomes) have been observed to accumulate in the brains of patients with Alzheimer's disease and other neurodegenerative diseases.<sup>4,5</sup> Interestingly, attempts to restore lysosomal proteolysis and enhance autophagy in mouse models of Alzheimer's disease have shown positive effects on neuronal function and cognitive performance.<sup>5</sup>

**Contributing Institution:** Tri-Institutional Laboratory of Comparative Pathology, Memorial Sloan-Kettering Cancer Center, Weill Cornell Medical College, and The Rockefeller University, New York, NY 10065.

**References:**

1. Frosch MP, Anthony DC, De Girolami U. The central nervous system. In: Kumar V, Abbas AK, Fausto N, Aster JC, eds. *Robbins and Cotran Pathologic Basis of Disease*. 8<sup>th</sup> ed. Philadelphia, PA: Saunders Elsevier; 2010:1279-1344.
2. Oakley H, Cole SL, Logan S, et al. Intraneuronal amyloid aggregates, neurodegeneration, and neuron loss in transgenic mice with five familial Alzheimer's disease mutations: potential factors in amyloid plaque formation. *J Neurosci*. 2006;26:10129-10140.

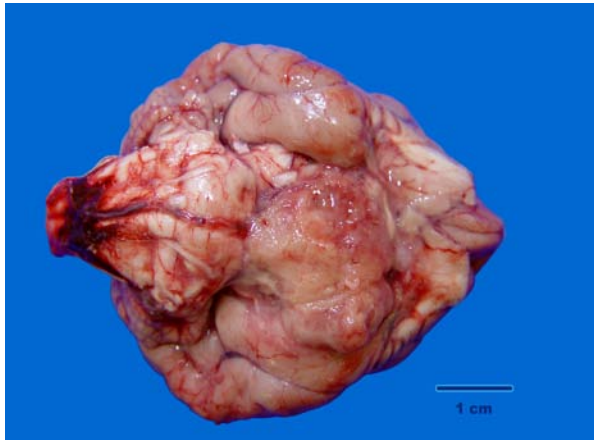
3. Gibbs G. Alois Alzheimer: The Man. [http://www.unmc.edu/intmed/geriatrics/docs/alois\\_alzheimer.pdf](http://www.unmc.edu/intmed/geriatrics/docs/alois_alzheimer.pdf) Accessed 19 October 2012.
4. Levine B, Kroemer G. Autophagy in the pathogenesis of disease. *Cell*. 2008;132(1):27-42.
5. Nixon RA, Yang DS. Autophagy failure in Alzheimer's disease—Locating the Primary Defect. *Neurobiol Dis*. 2011; 43(1):38-45.

**CASE III: C-16154-08 (JPC 3134053).**

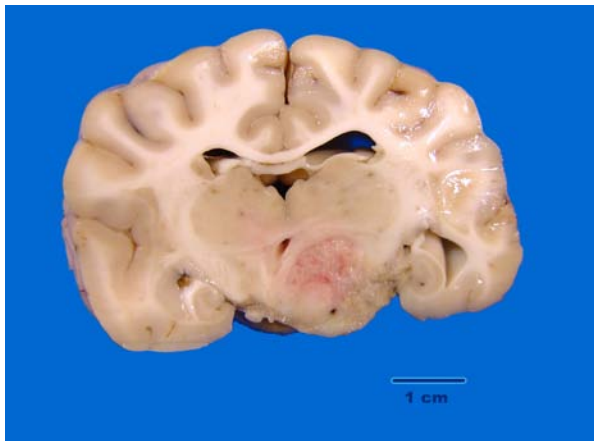
**Signalment:** 5-year-old, male/castrated, American Pit Bull Terrier, dog, *Canis familiaris*.

**History:** The dog had a two week history of listlessness and decreased appetite. When examined at the clinic, the animal was dehydrated, lethargic, showing neurological signs (standing in the corner staring at the wall) and had anisocoria. Pain was elicited on flexion and extension of the neck. An intracranial mass was suspected and the owners opted to euthanize the dog.

**Gross Pathologic Findings:** The carcass is in good body condition; significant changes are restricted to the



3-1. Cerebrum, hypothalamus: A soft, pink, irregular mass measuring approximately 1 x 2 x 2 cm is present on the ventral surface of the brain, centered over the diencephalon slightly to the left of midline (image 1). (Photo courtesy of: Department of Pathology and Microbiology, Atlantic Veterinary College, University of Prince Edward Island, 550 University Avenue, Charlottetown, PE C1A 4P3, <http://www.upei.ca/~avc/index.html>)

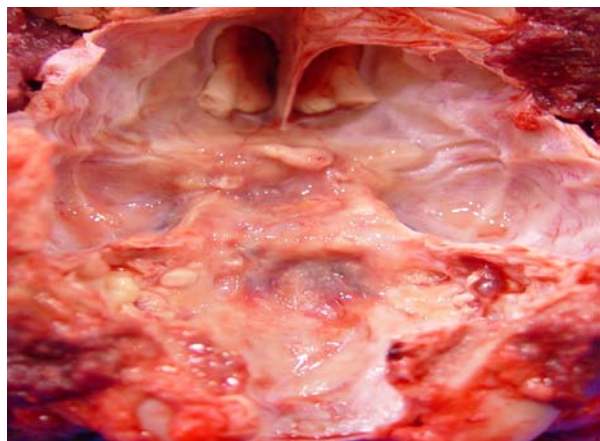


3-2. On cut section, the mass infiltrates and compresses the hypothalamus, thalamus, piriform lobe and the hippocampus. (Photo courtesy of: Department of Pathology and Microbiology, Atlantic Veterinary College, University of Prince Edward Island, 550 University Avenue, Charlottetown, PE C1A 4P3, <http://www.upei.ca/~avc/index.html>)

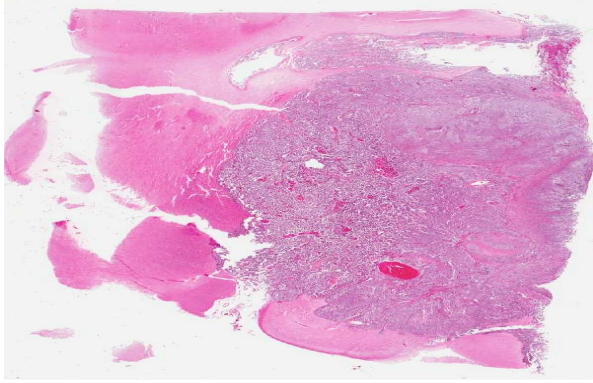
brain/skull base. A soft, pink, irregular mass measuring approximately 1 x 2 x 2 cm is present on the ventral surface of the brain, centered over the diencephalon slightly to the left of midline. The mass extends caudally from the olfactory tract to the rostral margin of the pons. Laterally the mass abuts the piriform lobe on the right and covers half of the piriform lobe on the left. On cut section, the mass infiltrates and compresses the hypothalamus, thalamus, piriform lobe and the hippocampus. The underlying floor of the skull appears irregular, thickened, and slightly yellow; the pituitary gland could not be identified.

**Laboratory Results:** Paraffin embedded tissue sections were sent to the Diagnostic Center for Population and Animal Health (Michigan State University). Sections were evaluated for Alpha-fetoprotein immunohistochemical markers. Approximately 60-70 % of the atypical cell population had strong positive cytoplasmic labeling with Alpha-fetoprotein.

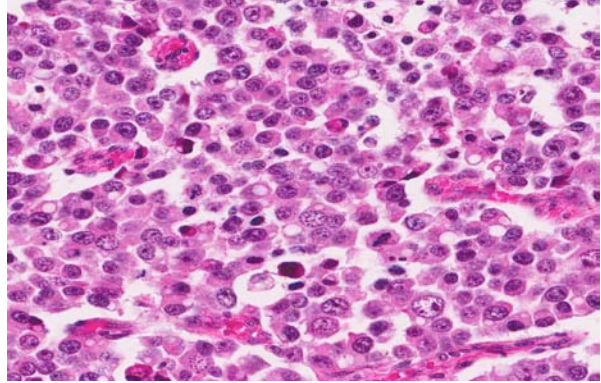
**Histopathologic Description:** A well-delineated, nonencapsulated, moderately cellular, multilobulated mass compresses and invades the neuropil of the thalamus, hypothalamus, hippocampus, piriform lobe, optic tract, and the pituitary gland (depending on the section). Three cell types comprise the mass. Nests and solid lobules of loosely packed neoplastic cells separated by fine collagenous septa predominate; these cells are round to polygonal with distinct cell margins, a scant to moderate amount of flocculent amphophilic cytoplasm and a central round nucleus with granular to coarsely clumped, often hyperchromatic, chromatin and an indistinct nucleolus. Scattered amongst these cells are discrete islands and trabeculae of large



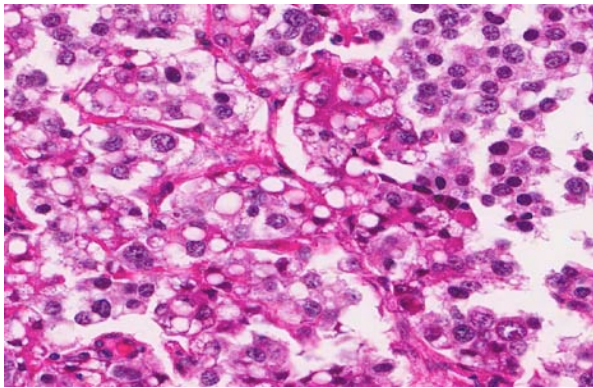
3-3. The underlying floor of the skull appears irregular, thickened, and slightly yellow; the pituitary gland could not be identified. (Photo courtesy of: Department of Pathology and Microbiology, Atlantic Veterinary College, University of Prince Edward Island, 550 University Avenue, Charlottetown, PE C1A 4P3, <http://www.upei.ca/~avc/index.html>)



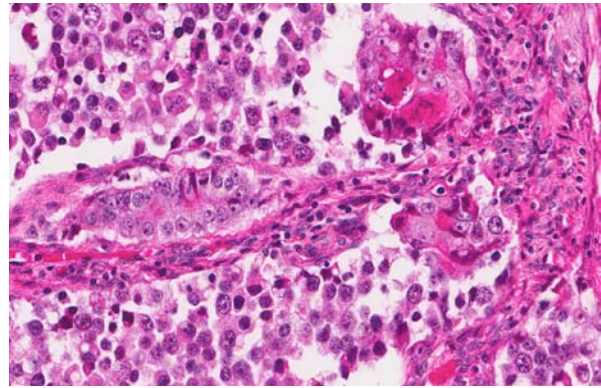
3-4. Cerebrum, thalamus: A large well-demarcated densely cellular neoplasm compresses the thalamus and overlying cerebrum. (HE 20X)



3-5. Cerebrum, thalamus: The majority of the neoplasm is composed of round germ cells and are arranged in sheets and nests on a fine fibrovascular stroma. (HE 224X)



3-6. Cerebrum, thalamus: A second, less common cell type, is similar to the neoplastic germ cells, but contains a single large clear vacuole. Rarely, these cells may exhibit squamous differentiation. (HE 260X)



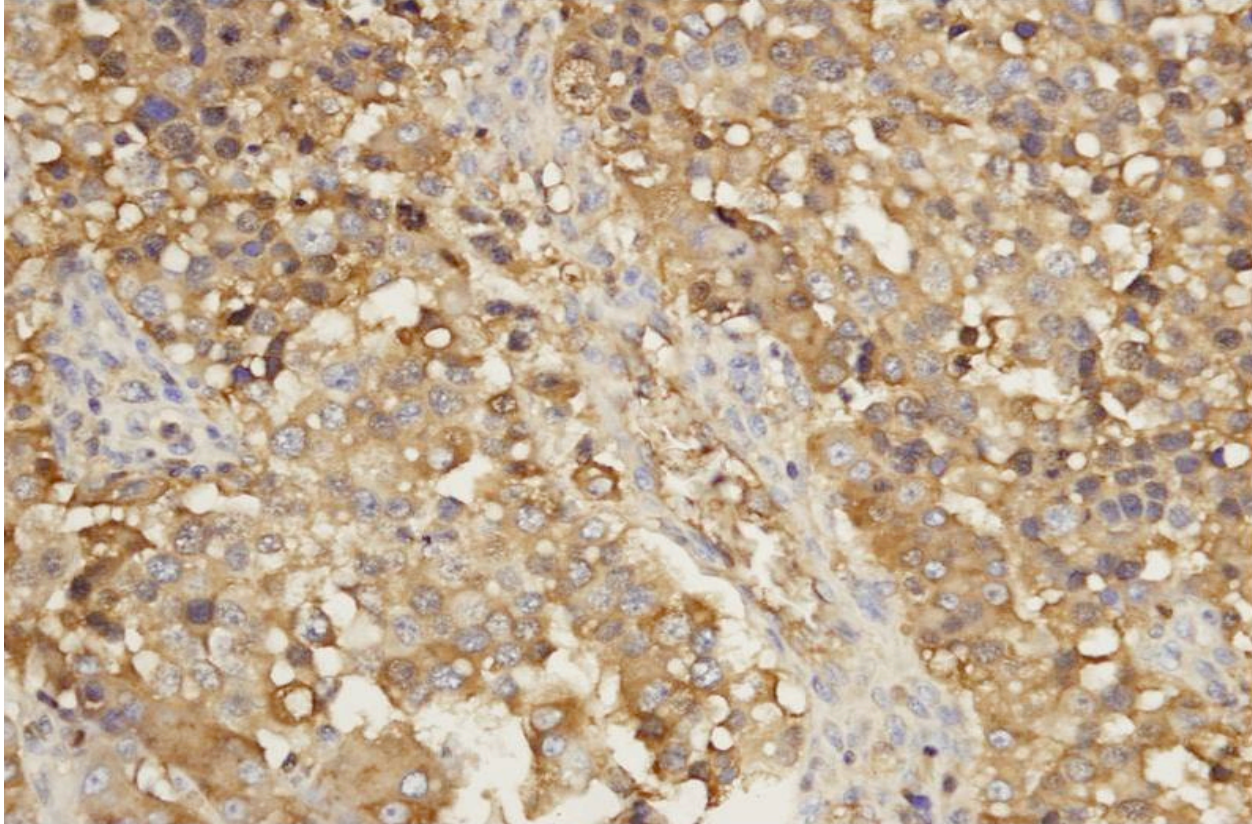
3-7. Cerebrum, thalamus: Rare trabeculae of neoplastic cuboidal to columnar cells are scattered throughout the neoplasm, rarely forming acinar-like structures. (HE 260X)

polygonal cells with moderate amounts of eosinophilic cytoplasm and a large oval vesicular nucleus with a single distinct nucleolus; these cells often contain discrete cytoplasmic vacuoles which displace the nucleus to the periphery or, less often, exhibit squamous differentiation. Rare aggregates of tubule-like structure lined by one to multiple layers of cuboidal to columnar epithelial cells with basal nuclei, granular chromatin and single to multiple nucleoli comprise the third population (not present in all slides). There is moderate anisocytosis and anisokaryosis. Mitoses, which are largely restricted to the round cells, average between 2 and 3 per HPF (40X). Small to moderate numbers of lymphocytes form multifocal aggregates within the supporting stroma, often surrounding blood vessels. Variably sized foci of necrosis and/or hemorrhage are scattered throughout the mass and rare mineral deposits and intravascular fibrin thrombi are noted.

**Contributor's Morphologic Diagnosis:** Malignant mixed germ cell tumor, brain (Canine suprasellar germ cell tumor).

**Contributor's Comment:** Tumors in the sellar region of the canine brain include pituitary tumors, craniopharyngioma, and suprasellar germ cell tumor.<sup>8</sup> Histological features in this case were not compatible with a pituitary tumor. Suprasellar germ cell tumors may be misclassified as craniopharyngioma, and this diagnosis was considered in this case.<sup>6,14</sup> A diagnostic feature of craniopharyngioma in humans is an epithelial component consisting of outer palisading columnar cells with central stellate cells resembling ameloblastoma; this characteristic was not observed in this mass.<sup>10,14</sup>

A diagnosis of suprasellar germ cell tumor was made based on three criteria: (1) midline suprasellar location, (2) presence within the tumor of several distinct cell types; one population resembling seminoma or dysgerminoma and others suggesting teratomatous differentiation into secretory glandular and squamous elements, and (3) positive staining for alpha-fetoprotein.<sup>14</sup> Alpha-fetoprotein is a commonly used marker for germ cells in human and has been shown to be a useful marker for canine intracranial germ cell tumors.<sup>14</sup>



3-8. Cerebrum, thalamus: Neoplastic cells show multifocal moderate to strong cytoplasmic positivity for alpha-fetoglobulin. (AFG 400X) (Photo courtesy of: Department of Pathology and Microbiology, Atlantic Veterinary College, University of Prince Edward Island, 550 University Avenue, Charlottetown, PE CIA 4P3, <http://www.upei.ca/~avc/index.html>)

Germ cell tumors most commonly occur in the ovaries and testes (dysgerminomas and seminomas respectively). Extragonadal germ cell tumors, with similar histology, are reported less commonly and typically occur on midline, affecting the mediastinum, brain, and coccyx in humans.<sup>13</sup> In dogs, these rare tumors have been reported in the brain, the eye, and the spinal cord.<sup>5,10,11,12,14</sup> Intracranial germ cell tumors tend to localize in the pineal and suprasellar regions in humans, while the suprasellar region is preferentially affected in dogs.<sup>14</sup> Suprasellar germ cell tumors have also been described in three lake whitefish (*Coregonus clupeaformis*).<sup>9</sup>

Presenting clinical signs in affected dogs include visual disturbance, pupil abnormality, lethargy, anorexia, and less often, signs of pituitary dysfunction.<sup>10,12,14</sup> Typically young adult dogs are affected and there is a possible breed predilection for the Doberman Pinscher.<sup>14</sup>

The pathogenesis of these tumors remains poorly understood, with the main question being the origin of the germ cells in the brain.<sup>6</sup> During embryonic development, progenitor germ cells originate in the epiblast. These germ cells then migrate to the caudal yolk sac endoderm and reach the gonadal ridge via the

dorsal mesentery of the hindgut. Extragonadal germ cell tumors are presumed to arise from ectopic embryonic germ cells which may become displaced during development, survive physiologic dissolution, and undergo neoplastic transformation.<sup>3,6</sup>

**JPC Diagnosis:** Cerebrum: Suprasellar germ cell tumor.

**Conference Comment:** The contributor provided a very good summary of suprasellar germ cell tumors. In describing the key features of this tumor, the contributor noted the midline suprasellar location as one of three criteria used for diagnosis. "Suprasellar" refers to the location above the sella turcica, a bony complex in the basisphenoid formed by the tuberculae sellae, the hypophyseal fossa, and the dorsum sellae with its two clinoid processes.<sup>3</sup> The sella turcica houses the hypophysis. In dogs, this shallow fossa is lined by the endosteal layer of dura mater. The meningeal layer of the dura mater forms the diaphragm sellae, which extends partially over the dorsal aspect of the fossa to form an incomplete septum.<sup>5</sup>

Recently, a supracellar germ cell tumor was described in a 16-month-old Wagyu heifer calf adding to the list

of species affected.<sup>1</sup> In the human literature, intracranial germ cell tumors have been divided into germinoma, teratoma, yolk sac tumor, embryonal carcinoma, and choriocarcinoma. Mixed germ cell tumors contain elements from more than one of these types.<sup>2</sup>

Conference participants noted there was significant slide variation, with some slides having polygonal neoplastic cells forming tubular structures, while others lacked these features. In addition, due to slide variation, the participants chose the generic location “cerebrum” for the morphologic diagnosis, as specimens varied in their anatomic location.

**Contributing Institution:** Department of Pathology and Microbiology, Atlantic Veterinary College, University of Prince Edward Island, 550 University Avenue, Charlottetown, PE C1A 4P3, <http://www.upei.ca/~avc/index.html>.

#### References:

1. Brooks AN, Brooks KN, Oglesbee MJ. A suprasellar germ cell tumor in a 16-month-old Wagyu heifer calf. *J Vet Diag Invest.* 2012;24:587-590.
2. Burger PC, Scheithauer BW. *Tumors of the Central Nervous System.* Third series, Fascicle 10. Washington, DC: Armed Forces Institute of Pathology/ American Registry of Pathology. 1993:251-257.
3. Echevarria ME, Fangusaro J, Goldman S. Pediatric central nervous system germ cell tumors: a review. *The Oncologist.* 13: 690 -699, 2008.
4. Evans HE. The skull. In: Evans HE, ed. *Miller's Anatomy of the Dog.* Philadelphia, PA: WB Saunders Company; 1993:139.
5. Ferreira AJA, Peleteiro MC, Carvalho T, et al. Mixed germ cell tumor of the spinal cord in a young dog. *J Small Anim Pract.* 2003;44:81-84.
6. Hoei-Hansen CE, Sehested A, Juhler M, et al. New evidence for the origin of intracranial germ cell tumors from primordial germ cells: expression of pluripotency and cell differentiation markers. *J Pathol.* 2006;209:25-33.
7. Hullinger RL. The endocrine system. In: Evans HE, ed. *Miller's Anatomy of the Dog.* Philadelphia, PA: WB Saunders Company; 1993:139, 561.
8. Maxie MG, Youseff S. Neoplastic diseases of the nervous system. In: Maxie MG, ed. *Jubb, Kennedy and Palmer's Pathology of Domestic Animals.* Vol. 1. 5<sup>th</sup> ed. Philadelphia, PA: Saunders Elsevier Limited; 2007:446-457.
9. Mikaelian I, Lapointe J-M, de Lafontaine Y, et al. Suprasellar germinoma in three lake whitefish (*Coregonus clupeaformis*). *Acta Neuropathol.* 2000;100: 228-232.
10. Nyska A, Harmelin A, Baneth G, et al. Suprasellar differentiated germ cell tumor in a male dog. *J Vet Diagn Invest.* 1993;5:462-467.
11. Patterson-Kane JC, Schulman FY, Santiago N, et al. Mixed germ cell tumor in the eye of a dog. *Vet Pathol.* 2001;38:712-714.
12. Rech RR, de Souza SF, da Silva MC, et al. Suprasellar germ cell tumor in a dog. *Ciencia Rural.* 2008;38:830-832.
13. Schneider DT, Schuster AE, Fritsch MK, et al. Multipoint imprinting analysis indicates a common precursor cell for gonadal and nongonadal pediatric germ cell tumors. *Cancer Research.* 2001;61:7268-7276.
14. Valentine BA, Summers BA, de Lahunta A, et al. Suprasellar germ cell tumors in the dog: a report of five cases and review of the literature. *Acta Neuropathol.* 1988;76:94-100.

**CASE IV: K09-038255 (JPC 3167327).**

**Signalment:** 4.5-year-old spayed female domestic ferret, *Mustela putorius furo*.

**History:** The ferret was presented as an emergency to a local veterinary clinic for dyspnea. The ferret was treated with intravenous fluids, Baytril, Cefazolin, Amoxicillin and oxygen, then euthanized after review of thoracic radiographs.

**Gross Pathologic Findings:** All lung lobes were similarly affected: pale, mottled, with a firm texture, and patchy red areas on cut section. Mediastinal lymph nodes were enlarged.

**Laboratory Results:** PCR for influenza virus was negative.

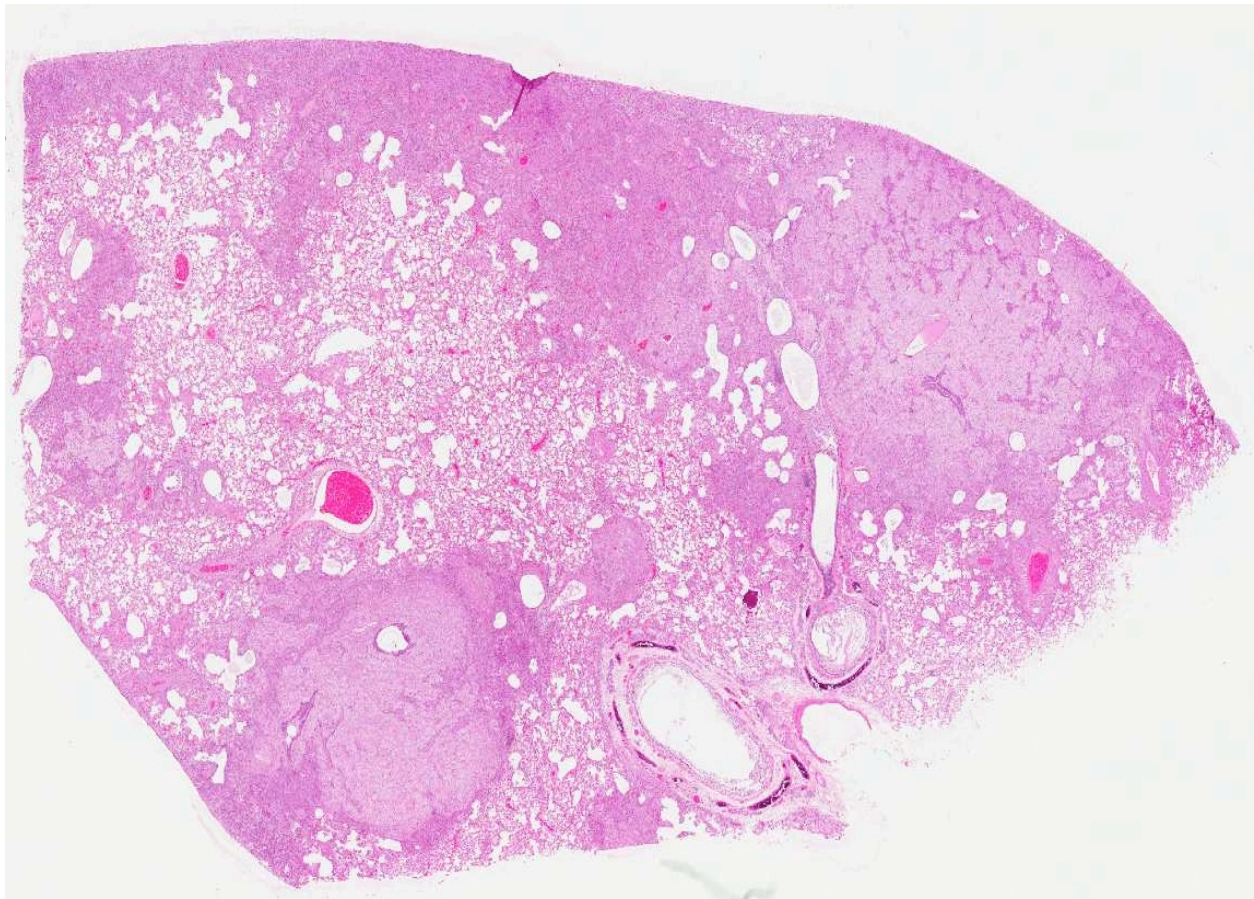
**Histopathologic Description:** Pulmonary architecture is distorted by locally extensive, alveolar infiltrates of eosinophilic foamy material, which on higher power examination is composed of myriad approximately 4-10 micron diameter discrete round or oval structures with thin eosinophilic outlines (which stain with Gomori's methenamine silver) and unstained content

except for one or more tiny 0.5 micron central basophilic bodies. These infiltrates are located predominantly in subpleural, peribronchiolar, perivascular and intramural vascular locations. Surrounding these areas is a more generalized alveolar infiltrate of large foamy macrophages, many of which contain similar organisms, admixed with moderate numbers of multinucleated giant cells, and lesser numbers of lymphocytes, plasma cells, neutrophils, with alveolar edema and focal fibrin exudation.

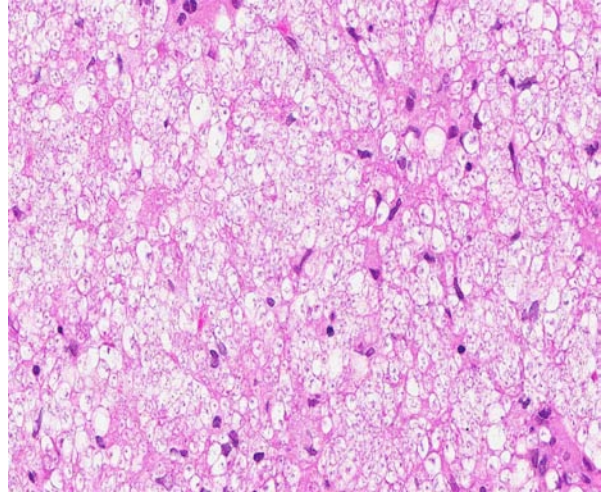
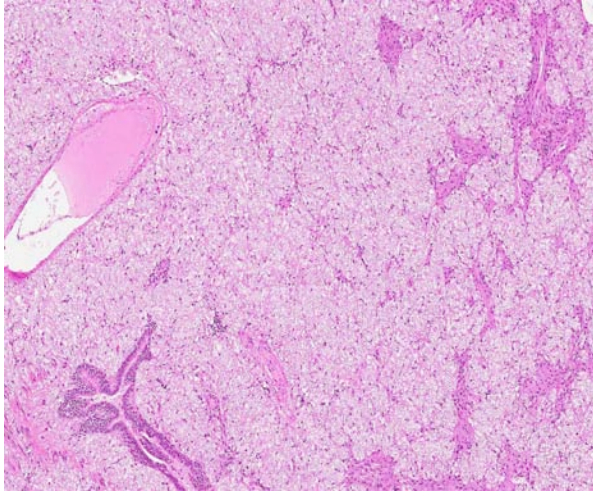
Similar infiltrates were present in the enlarged mediastinal lymph nodes and spleen (sections not provided).

**Contributor's Morphologic Diagnosis:** Severe, subacute granulomatous interstitial pneumonia with infiltrates of organisms morphologically consistent with *Pneumocystis*.

**Contributor's Comment:** *Pneumocystis* spp. are inhabitants of the lung of various domestic and laboratory animal species including ferrets, pigs, foals, dogs, rats, mice, non-human primates as well as humans.<sup>1,2</sup> Originally thought to be a protozoan, *Pneumocystis* is now classified as a fungus, likely an



4-1. Lung, ferret: Approximately 50% of the alveoli, especially in subpleural areas, are filled with exudate. (HE 4X)



4-2, 4-3. Lung, ferret: Alveoli are filled with a flocculent exudate comprised of low numbers of macrophages and neutrophils and numerous intra- and extracellular fungal organisms consistent with *Pneumocystis carinii*. (HE 60X, 300X)

early divergent lineage of the genus *Ascomycetes*.<sup>1</sup> The organism is considered an opportunistic pathogen, and development of clinical disease usually requires immunosuppression, either by concurrent disease or the use of immunosuppressive drug therapy.

There are significant genomic, karyotypic, isoenzymatic and antigenic differences among the *Pneumocystis* species isolated from different animal hosts, and there appears to be close hostspecificity.<sup>1</sup> The taxonomy of these organisms has undergone significant changes in the last decade, and the organisms originally classified as *Pneumocystis carinii* include various divergent strains now recognized as unique species, including *Pneumocystis jirovecii* which colonizes humans, *P. wakefieldiae* which together with the original *P. carinii* has been found in the Norway rat, *P. murina* in laboratory mice and *P. oryctolagi* in Old World rabbits. Genetically distinct populations of *Pneumocystis* have been also been recognized in the ferret, and may represent multiple separate species, although these have not yet been completely characterized.<sup>6</sup>

*Pneumocystis* infection is thought to be maintained in host populations by airborne circulation, as the organism is capable of at least transiently colonizing and replicating in the lung of immunocompetent hosts, and can be spread between healthy hosts as well as to immunocompromised susceptible hosts.<sup>1</sup> In the lung, life cycle stages recognized include a 1-4 micron diameter, thin-walled vegetative or trophic form, which attaches to type 1 alveolar epithelial cells and appears to develop through three consecutive sporocyte stages to produce a 3-8 micron diameter, thick-walled cyst form, in which multiple nuclear divisions lead to the formation of eight intracystic spores.<sup>1</sup> These intracystic bodies are released and presumably develop

into trophic forms. (Note that the names of these stages still reflect the original classification of these organisms as protozoa; appropriate renaming of these stages as fungal developmental stages awaits further elucidation of the sexual stages of the cycle). Binding to type I pneumocytes as well as to macrophages is mediated by the cell wall major surface glycoprotein A. Both macrophages and cell-mediated immunity are important for control of infection, and development of clinical disease implies impairment of either macrophage function or cell-mediated immunity.<sup>2</sup>

The ferret has been used as an animal model of *Pneumocystis* pneumonia induced by corticosteroid administration, while development of disease in pet ferrets is recognized as a potential complication of long-term corticosteroid therapy or hyperadrenocorticism.<sup>3</sup> In this case, no predisposing condition was identified. Both adrenal glands were histologically unremarkable (although the right adrenal had a small intracortical cyst). Extrapulmonary localization of the organisms was apparent in this case, and has been reported in liver and kidney from 10% of experimentally immunosuppressed ferrets.<sup>6</sup>

**JPC Diagnosis:** Lung: Pneumonia, interstitial, histiocytic and necrotizing, diffuse, marked, with numerous intra-alveolar fungal cysts consistent with *Pneumocystis carinii*.

**Conference Comment:** The contributor provided a good summary of disease associated with *Pneumocystis* species. As stated, *Pneumocystis* can affect several species of animals, usually causing disease only in immunocompromised hosts. Interestingly, however, studies have linked *Pneumocystis carinii* to infectious interstitial pneumonia (IIP), a common, transient, usually mild

disease of immunocompetent laboratory rats that has been, until recently, attributed to an alleged virus referred to as rat respiratory virus (RRV). The distinctive lung lesions (lymphohistiocytic interstitial pneumonia with perivascular lymphocytic cuffs) associated with IIP, first described in the mid-1990s, led researchers to suspect a viral cause. Subsequent studies showed the presence of a virus that could be propagated in cell culture; this virus was referred to as RRV. However, the RRV antibody assays did not correspond to the IIP status of colonies as determined by histopathology, leaving histopathology as the only reliable diagnostic method for rat colony surveillance. Since then, several investigations have demonstrated a cause and effect relationship between *Pneumocystis carinii* and IIP in immunocompetent rat colonies using PCR and IFA, as well as histopathology. These studies also found that the concentration of *Pneumocystis carinii* in the lung corresponded with the histologic severity of IIP. Furthermore, clearance of *Pneumocystis carinii* lung infection via a humoral response corresponded with resolution of pneumonia. *Pneumocystis carinii* is the most common *Pneumocystis* species found in rats, occurring much more frequently than *Pneumocystis wakefieldiae*. *Pneumocystis wakefieldiae* was not found to be associated with IIP.<sup>4</sup>

**Contributing Institution:** Animal Health Laboratory,  
University of Guelph, Guelph, Ontario, Canada  
<http://ahl.uoguelph.ca>

**References:**

1. Aliouat-Denis C-M, Chabe M, Demanche C, et al. *Pneumocystis* species, co-evolution and pathogenic power. *Infect Genet Evol.* 2008;8:708-726.
2. Caswell JL, Williams KJ. Respiratory system. In: Maxie MG, ed. *Jubb, Kennedy, and Palmer's Pathology of Domestic Animals*. 5<sup>th</sup> ed. Philadelphia, PA: Saunders Elsevier; 2007:593.
3. Dei-Cas E, Brun-Pascaud M, Bille-Hansen V, et al. Animal models of pneumocystosis. *FEMS Immunol Med Microbiol.* 1998;22:163-168.
4. Henderson KS, et al. *Pneumocystis carinii* causes a distinctive interstitial pneumonia in immunocompetent laboratory rats that had been attributed to "rat respiratory virus." *Vet Pathol.* 2012;49: 440-452.
5. Oz HS, Hughes WT, Vargas SL. Search for extrapulmonary *Pneumocystis carinii* in an animal model. *J Parasitol.* 1996;82:357-359.
6. Wakefield AE. Genetic heterogeneity in *Pneumocystis carinii*: an introduction. *FEMS Immunol Med Microbiol.* 1998;22:5-13.